JOM, Vol. 71, No. 12, 2019
https://doi.org/10.1007/s11837-019-03605-6

Selective Nitric Acid Leaching of Rare-Earth Elements from Calcium and Phosphate in Fluorapatite Concentrate

SEYED RAMIN BANIHASHEMI,[1] BIJAN TAHERI ,[1,3]
SEYED MOHAMMAD RAZAVIAN,[1] and FARAZ SOLTANI[2]

1.—Department of Mining Engineering, University of Kashan, Kashan, Iran. 2.—Department of Mining Engineering, Arak University of Technology, Arak, Iran. 3.—e-mail: Bijan.taheri@kashanu.ac.ir

Esfordi phosphate concentrate (Yazd Province, Iran) contains 13.1% P, 34.6% Ca, and 1.09% rare-earth elements (REEs), being one of the most important sources of REEs in Iran. REEs can be extracted from phosphate concentrates as a by-product of phosphoric acid production processes. In this work, nitric acid was used for leaching of REEs and phosphate from Esfordi phosphate concentrate, and the effects of the acid concentration (35–65 wt.%), leaching time (30–90 min) and temperature (24–90°C) were investigated. Due to the difficulty of calcium separation from REEs in nitrate-phosphate solutions, the possibility of selective leaching of calcium and phosphate from REEs was examined. At acid concentration of 35%, temperature of 60°C, and leaching time of 70 min, most of the calcium, more than 80% of the phosphate, and less than 10% of the REEs were dissolved. Accordingly, 90.7% of the REEs remained in the residue and their grade was increased from 1% to 4% in the nitric acid leaching residue. This concentrated residue of REEs could be an appropriate feed for subsequent processes, including acid baking.

INTRODUCTION

The rare-earth elements (REEs) include 15 lanthanide elements, plus yttrium and scandium. REEs can be classified into two subgroups, viz. the light rare-earth elements (LREEs) from lanthanum to europium, and the heavy rare-earth elements (HREEs), which include the rest of the lanthanide elements along with yttrium.[1,2] The demand for REEs has spiked in recent years due to their increasing application in numerous high-technology fields, including high-strength permanent magnets, phosphors for electronic displays, various renewable energy technologies, and as alloying agents in metals.[3]

REEs are found in a variety of minerals such as silicates, halides, carbonates, and phosphates but never as pure metals. Notably mined rare-earth minerals are bastnäsite [$(La,Ce)FCO_3$], monazite [$(Ce,La,Y,Th)PO_4$], and xenotime [YPO_4].[3–5]

Separation and recycling of lanthanides from different secondary resources has recently drawn extensive attention due to the increasing demand for lanthanides and their compounds for use in different technological applications.[6] Some of the secondary rare-earth minerals include apatite, brannerite, euxenite, gadolinite, loparite, and uraninite.[7] Apatite mineral has the chemical formula $Ca_{10}(PO_4)_6(OH,F,Cl)$, being the main source of phosphate for phosphoric acid production.[8] Apatite is not a rare-earth mineral but rather a rare-earth-concentrating mineral. Rare-earth ions substitute calcium ions in the apatite lattice because of their similar ionic sizes. The rare-earth content of apatite is highly variable, ranging from trace amounts to over 10% [as rare-earth oxides (REO)]. Despite the low concentration of REEs in apatite, the huge volumes of apatite make this material a potential source for extraction of REEs.[7,9,10]

Dihydrate and hemihydrate processes are the most common methods applied for production of phosphoric acid from apatite, during which REEs can be extracted as a byproduct. One of the most important issues with the mentioned processes is the generation of huge amounts of gypsum, which is likely to be a radioactive compound and may cause

 (Published online June 19, 2019)

environmental problems.[11] For this reason, different mineral acids are used to leach phosphate and REEs from apatite concentrates.[12]

Hydrochloric acid is scarcely used industrially for extraction of REEs from apatite, being mainly used on the laboratory scale.[11,13] Nitric acid has also been used as a leaching agent for extraction of most of the REE content from the apatite lattice. The main chemical reaction occurring during dissolution of apatite using nitric acid can be represented as[14]

$$Ca_{10}(PO_4)_6F_2 + 20HNO_3 \rightarrow 6H_3PO_4 + 10Ca(NO_3)_2 + 2HF \quad (1)$$

When apatite is leached with HNO_3 or HCl, calcium does not precipitate due to the high solubility of calcium nitrate and calcium chloride.[15] Although nitric acid is expensive in comparison with sulfuric acid, its use can resolve the gypsum problem.[11] Moreover, HNO_3 can be recovered and used in a cyclic process.

Jorjani et al. (2011) and Stone et al. (2016) investigated the effects of the leaching time, acid concentration, and solid-to-liquid ratio on nitric acid leaching of REEs from apatite concentrate. The results of those studies indicated that increasing the acid concentration and leaching time combined with a decrease of the solid-to-liquid ratio could increase the efficiency of nitric acid for leaching of REEs.[9,11] Forsberg et al. (2014) investigated the leaching efficiency of Ce and Fe in 3 mol/L to 6 mol/L nitric acid in the temperature range of 60–80°C, concluding that the recovery of Ce could be increased by increasing the acid concentration from 3 mol/L to 5 mol/L. They also indicated that increasing the temperature from 60°C to 80°C did not have a significant effect on the Ce leaching efficiency.[16] Bandara and Senanayake (2015) studied the leaching efficiency of REEs, calcium, and minor metal ions from natural fluorapatite in different mineral acids. They declared that the leaching efficiency of REEs increased on prolonging the leaching time.[17]

In previous studies, selective leaching of calcium, phosphate, and REEs has not been investigated. The work presented herein therefore focuses on selective nitric acid leaching of REEs from Esfordi phosphate concentrate as a potential source of REEs in Iran; furthermore, the operating variables of acid concentration, reaction time, and temperature were optimized.

EXPERIMENTAL PROCEDURES

Esfordi Flotation Concentrate Sample

Esfordi ore is one of the most important iron-rich phosphate ores in the Bafq Region of Iran. As seen in the map in Fig. 1, the Esfordi plant is situated 35 km northeast of Bafq. In the Esfordi plant, a flotation technique is used to separate fluorapatite from associated gangue minerals.

A sample (250 kg, d_{80} = 55 μm) containing 1.09% REEs was obtained from the Esfordi flotation plant. The sample was riffled into 10-kg lots using a Jones riffler. It was further homogenized and riffled into 1000-g lots that were stored in polyethylene bags for further splitting by a Retsch® PT100 automatic sample divider just prior to experiments.

Optical mineralogy using polished and thin sections, x-ray diffraction (XRD) analysis, x-ray fluorescence (XRF) spectroscopy, and inductively coupled plasma-optical emission spectrometry (ICP-OES) were applied for characterization of the concentrate sample.

Leaching Experiments

Leaching experiments were carried out in a stirring 1-L glass reactor on a digital hot plate using reagent-grade nitric acid from Merck Millipore company and deionized water as leaching solution with solid-to-liquid ratio of 30%, agitation rate of 1000 rpm, and particle size (d_{80}) of 55 μm. In each leaching experiment, 100 g phosphate concentrate was added to the leaching solution when the temperature reached the preset value. The effects of the acid concentration (35–65%), temperature (57–90°C), and reaction time (30 min to 90 min) on the leaching efficiency of REEs (Y, Ce, La, and Nd) and phosphate were investigated. At the end of each leaching experiment, the pulp was filtered, and the solid residue was washed several times with hot water and dried at 105°C to constant weight. The pregnant leach solution and wash solutions were combined for assay. All solid and liquid samples were analyzed to calculate the leaching efficiency using Eq. 2 and the mass balance using Eq. 3:

$$\text{Leaching efficiency of metal } m(\%) = \left(\frac{C_m \times V_s}{M_f \times g_m}\right) \times 100 \quad (2)$$

$$(C_m \times V_s) + (M_r \times R_m) = (M_f \times g_m) \quad (3)$$

where C_m is the concentration of metal m in solution (mg/L), V_s is the solution volume (L), M_f denotes the weight of leached concentrate (kg), g_m represents the concentration of metal m in the concentrate (mg/kg), M_r stands for the weight of leaching residue (kg), and R_m is the concentration of metal m in the leaching residue (mg/kg).

Design of Experiments

Response surface methodology (RSM)-based design of experiments can determine the optimum process conditions using the minimum number of experiments, avoiding the need to study all possible parameter combinations. In the RSM, a response or a combination of responses (leaching efficiency of phosphate and REEs) is influenced by input variables (leaching time, leaching temperature, and acid concentration) and the aim is to optimize the

Fig. 1. Location of Esfordi plant.

mentioned response. Thus, finding an appropriate (first- or second-order) model to describe the relationship between each response and the input variables is the first step in experimental design by RSM. If a linear function is used to describe the best relationship between the response and input variables, the model is called first order. A polynomial function of higher degree can be used when there is curvature in the system response.[18] The quadratic (second-order) model shown in Eq. 4 was used to design the mineral processing experiments:[19]

$$Y = \beta_0 + \sum_{i=1}^{k} \beta_i x_i \sum_{<i<j}^{k} \beta_{ii} x_i^2 + \sum_{1<i<j}^{k} \beta_{ij} x_i x_j + \varepsilon \qquad (4)$$

where k is the number of variables, β_0 is a constant, β_i are the linear coefficients, x_i are the variables, β_{ii} are the quadratic parameters, β_{ij} are the interaction coefficients, and ε is the residual error related to the experiments.[18,19]

Central composite design (CCD) is the most common RSM approach, comprising the following parts: (1) a factorial design including all possible combinations of the high and low levels of the factors, (2) experimental points at a distance of α from the center point (called axial points), and (3) a center point, referring to the midpoint of each factor range, e.g., for example, 57°C for the temperature factor (Table I).[18]

Using these levels and standard statistical software (DX7 or Matlab), sufficient information can be

generated to fit the model to the data. DX7 (Design-Expert®, version 7) is a powerful and easy-to-use program for design of experiments (DOE), developed by Carol Kavanaugh, C.F. Kavanaugh & Associates (Kingston, Ontario, Canada). In this study, the fit quadratic models were used to find the optimum leaching efficiency of REEs and phosphate.

According to preliminary tests and previous studies,[15,20] the effects of the acid concentration, temperature, and reaction time on the leaching efficiency of REEs (Ce, La, Nd, and Y) and phosphate were investigated using the CCD method. The actual and coded levels of the independent variables in the CCD design are presented in Table I. The experiments were designed using DX7 software.

RESULTS AND DISCUSSION

Esfordi Flotation Concentrate

The results of elemental analysis of the Esfordi phosphate concentrate are presented in Table II, revealing that the concentrate sample contained 34.6% Ca, 13.1% P, 2.58% Fe, and 1.09% REEs. As seen in Fig. 2, the concentrate contained 15 rare-earth elements, among which light rare-earth elements including lanthanum, cerium, and neodymium and the heavy rare-earth element yttrium were the most prominent. Cerium, lanthanum, neodymium, and yttrium accounted for 88% of the total rare-earth content of the phosphate concentrate.

XRD analysis of the Esfordi sample (Fig. 3) revealed fluorapatite, hematite, and calcite as the main minerals and fluorapatite as the dominant mineral. Other minor phases present in the concentrate included magnetite, montmorillonite, calcite, talc, and quartz. The main REE-bearing minerals in Esfordi concentrate are fluorapatite, monazite, and xenotime. Fluorapatite is the chief mineral of the concentrate, and its ratio to monazite/xenotime is greater than 60.[15]

Model and Statistical Analysis

The data obtained from the leaching experiments (Table III) were statistically analyzed using analysis of variance (ANOVA) to identify the significant main and interaction effects of the factors (Table IV). By applying multiple regression analysis, the quadratic or 2FI polynomial models were fit to the experimental results.

Table I. Actual and coded levels of independent variables used in CCD design

No.	Variable	Unit	Symbol code	Coded levels		
				− 1	0	+ 1
1	Temperature	°C	A	24	57	90
2	Reaction time	min	B	30	60	90
3	Acid concentration	wt%	C	35	50	65

Table II. Elemental analysis of concentrate sample

Major elements		Minor elements		Rare earths	
Element	Mass percentages (%)	Element	ppm (mg/kg)	Element	ppm (mg/kg)
Ca	34.6	Si	7610	Ce	4590
P	13.1	Mg	2413	Nd	2175.7
Fe	2.58	Na	1481	La	2138
F	2.86	Al	593	Y	667.1
Cl	0.33	S	716	Pr	397.2
		Sr	414.6	Sm	348.9
		Ti	130	Dy	126.8
		K	< 100	Er	55.6
		V	106	Eu	28.5
		Mn	121	Lu	4.1
		Th	75.01	Tb	33.9
		U	4.6	Yb	46.2
				Gd	235.3
				Ho	24.2
				Tm	5.87

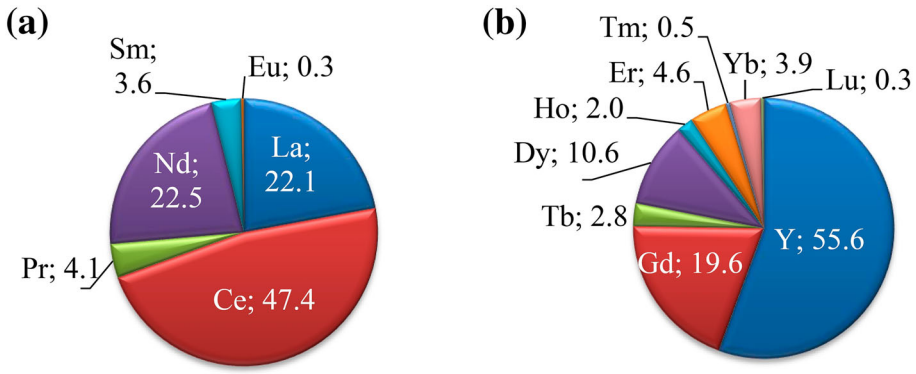

Fig. 2. Distribution of (a) light and (b) heavy rare-earth elements in Esfordi flotation concentrate sample.

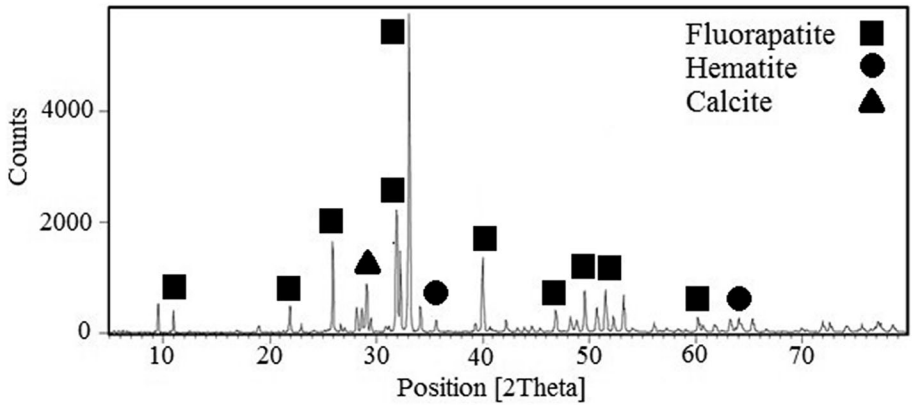

Fig. 3. XRD analysis of Esfordi sample.

Table III. Results of nitric acid leaching experiments

Run	Factors			Leaching efficiency (%)				
	A: Temperature (°C)	B: Reaction time (min)	C: Acid concentration (wt.%)	Ce	La	Nd	Y	P
1	24	30	35	0.6	0.6	0.6	0.4	65.2
2	90	30	35	18.2	16.2	17.5	14.1	81.3
3	24	90	35	2.5	2.4	2.5	2.2	70.2
4	90	90	35	29.2	29.0	28.7	25.2	90.0
5	24	30	65	15.1	15.1	15.3	11.6	75.4
6	90	30	65	31.0	29.9	30.2	29.0	88.1
7	24	90	65	25.0	23.1	23.5	18.1	73.1
8	90	90	65	40.3	40.0	39.8	33.5	89.5
9	24	60	50	8.9	7.6	7.7	5.9	73.5
10	90	60	50	31.6	31.9	32.1	30.7	85.5
11	57	30	50	10.8	11.6	11.4	5.1	79.6
12	57	90	50	21.7	20.8	20.8	13.8	83.1
13	57	60	35	9.0	8.2	8.6	5.6	83.4
14	57	60	65	28.2	27.9	27.9	25.3	84.6
15	57	60	50	17.5	18.9	16.9	11.7	83.0
16	57	60	50	18.2	17.8	18.1	12.1	82.0
17	57	60	50	17.3	16.5	17.2	13.1	83.1
18	57	60	50	19.1	17.9	18.8	11.3	81.6
19	57	60	50	19.2	18.2	18.9	12.8	81.2
20	57	60	50	18.7	18.0	18.2	10.3	83.3

Table IV. ANOVA results of the responses

Statistical results	Response 1: (Ce leaching efficiency)	Response 2: (La leaching efficiency)	Response 3: (Nd leaching efficiency)	Response 4: (Y leaching efficiency)	Response 5: (P leaching efficiency)
Model	RQuadratic	R2FI	R2FI	RQuadratic	RQuadratic
Model F value	403.11	307.82	352.76	150.35	56.76
Model prob > F	< 0.0001	< 0.0001	< 0.0001	< 0.0001	< 0.0001
Lack of fit F value	2.41	4.38	3.42	3.49	4.68
Lack of fit P value	0.1729	0.0583	0.0934	0.0937	0.0520
R-squared	0.9931	0.9880	0.9895	0.9887	0.9530
Adj. R squared	0.9906	0.9848	0.9867	0.9822	0.9362
Pred. R squared	0.9829	0.9736	0.9801	0.8957	0.8728
SD	0.13	0.17	0.16	0.14	1.62
Mean	4.17	4.11	4.12	2.36	80.83
CV %	3.12	4.05	3.77	5.78	2.01
Adeq. precision	81.924	70.455	74.934	48.897	26.096

The relationships between the leaching efficiency of Ce, La, Nd, Y, and P (responses) and the input variables (Eqs. 5–9) were developed based on Eq. 4 and the results of the ANOVA (Table IV). Nonsignificant terms were eliminated from the fit models.

According to Table IV the models are significant, with only a 0.01% chance of the occurrence of such large model F-values due to noise. The "prob > F" values for all models are < 0.0001 (p value < 0.05), indicating that they are statistically significant with a confidence interval of 95%. Also the "pred R-squared" is in reasonable agreement with the "adj. R-squared," which can be regarded as another positive point. The "adeq. precision" measures the signal-to-noise ratio, with a ratio greater than 4 being desirable; the values in this table again support the fitness of the models.

$$\text{Sqrt (Ce leaching efficiency)} = 4.26 + 1.3A + 0.52B + 1.11C - 0.53AC - 0.18B^2 \quad (5)$$

$$\text{Sqrt (La leaching efficiency)} = 4.11 + 1.3A + 0.51B + 1.12C - 0.50AC \quad (6)$$

$$\text{Sqrt (Nd leaching efficiency)} = 4.12 + 1.31A + 0.49B + 1.10C - 0.52AC \quad (7)$$

$$\text{Ln (Y leaching efficiency)} = 2.5 + 0.92A + 0.38B + 0.8C - 0.18AB - 0.56AC - 0.21BC - 0.27B^2 \quad (8)$$

$$\text{P leaching efficiency} = 82.49 + 7.72A + 1.63B + 2.07C - 1.8BC - 3.32A^2 \quad (9)$$

where A, B, and C are the leaching temperature, leaching time, and acid concentration, respectively, while AB, AC, and BC denote the interactions between A, B, and C.

As shown in Eqs. 5–9, all three factors had positive effects on the leaching efficiency of Ce, La, Nd, Y, and P. Among the three factors, temperature was the most effective, as shown by its greater coefficient in the fit models. Amongst the interactions, AC had the greatest effect on the leaching of LREEs (Ce, La, and Nd), while the impact of the temperature–time and temperature–acid concentration interactions on the leaching efficiency of Y was negative. Unlike for the REEs, the effect of the interaction effect between the variables B and C on phosphate leaching was negative. As indicated by Eqs. 5–8, the square root (Sqrt) and natural log (Ln) were adequate transformations for the LREEs and HREEs, respectively.

Effect of Operating Variables

Effect of Leaching Temperature

The effect of the leaching temperature was studied in the range of 24–90°C using different leaching times and acid concentrations. The temperature factor had the strongest effect, as shown in the empirical Eqs. 5–9. It is evident that the leaching efficiencies of REEs and phosphate were increased by increasing the leaching temperature. Esfordi phosphate concentrate mainly contains fluorapatite, monazite, and xenotime as rare-earth minerals.[20] It can be concluded that, by increasing the leaching temperature above 60°C, almost all the REEs substituting calcium ions in the fluorapatite lattice can be leached.[21] The concentrate contained 2.86% fluoride, originating from the fluorapatite mineral (Table II). Fluoride can form strong complexes with

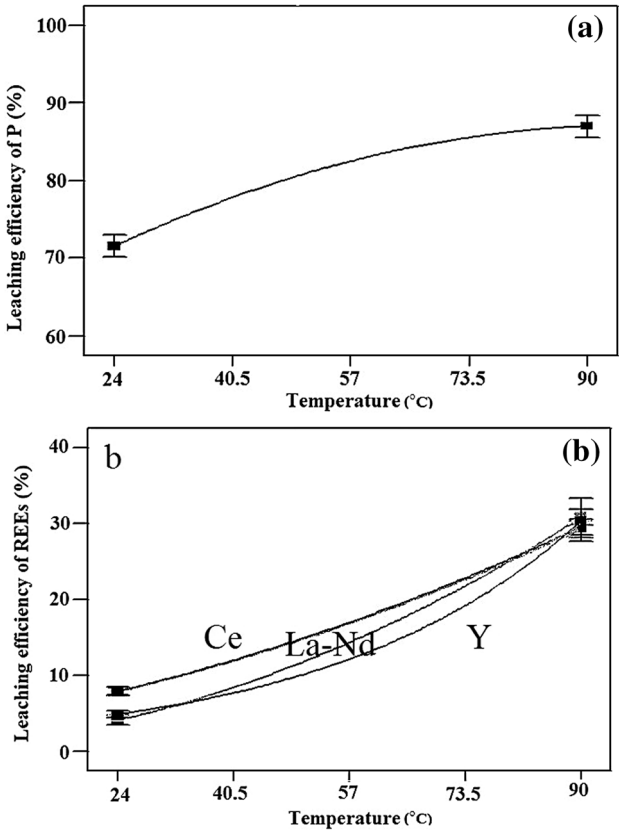

Fig. 4. Effect of leaching temperature on leaching efficiency of (a) P and (b) REEs (acid concentration 50%, time 60 min). Curves indicate regression models.

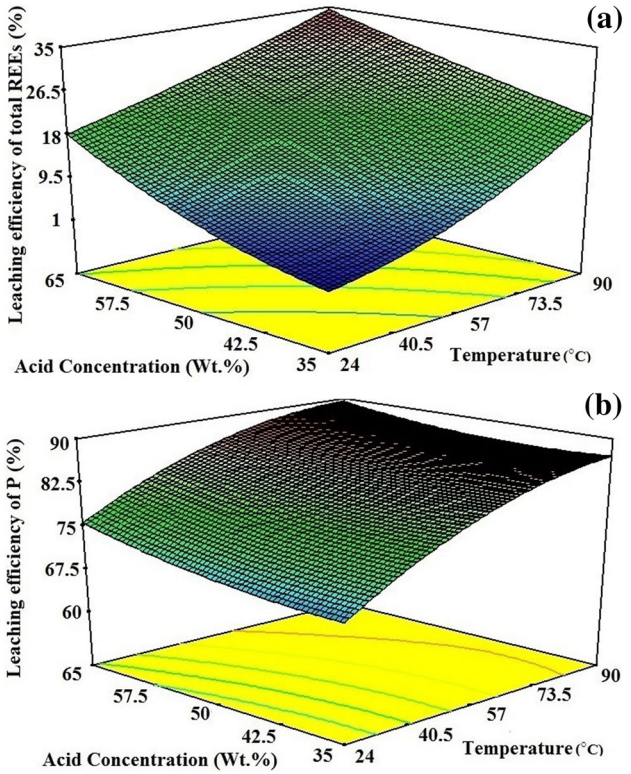

Fig. 5. Effect of the interaction between temperature and acid concentration on the leaching efficiency of (a) total REEs and (b) phosphate (leaching time 60 min). Curves indicate regression models.

REEs. It can be concluded that addition of fluoride ion to REE-containing nitric acid solution can cause precipitation of REEs in the form of fluorides.[22] It should be emphasized that fluoride is volatilized as HF (g) at temperatures above 60°C.[21] Thus, precipitation of REEs in the form of fluorides could be a reason for the lower leaching efficiency of REEs at lower temperatures.

As shown in Fig. 4a and b, the leaching efficiency of phosphate was much higher than that of REEs, which can be attributed to the important fact that about 60% of the REEs originate from refractory monazite and xenotime minerals [20] and thus cannot be attacked by HNO_3 at low temperatures (< 100°C).[3] Under the same conditions, a large portion of the fluorapatite (as the main source of calcium and phosphate) is dissolved in HNO_3.

The leaching efficiency of total REEs increased from 16.4% to 27.6% on increasing the temperature from 60°C to 90°C. However, this temperature elevation also increased the leaching efficiency of phosphate from 82.8% to 87% (Fig. 4). The coefficients of the factor *A* (leaching temperature) in Eqs. 5–9 indicate a greater impact of temperature on the leaching efficiency of REEs compared with the other factors. It should be emphasized that monazite and xenotime minerals are often decomposed by two conventional methods: sulfuric acid baking in the temperature range of 200–220°C and alkali treatment at about 140°C.[7] Thus, the leaching efficiency of REEs will continue to be enhanced as the temperature is increased, which is not favorable for selective leaching of phosphate and calcium from REEs.

Effect of Nitric Acid Concentration

The effect of the nitric acid concentration was also investigated in the range of 35–65 wt.%. As depicted in Eqs. 5–9, the acid concentration is the second most important factor for the REE and phosphate leaching efficiencies. Moreover, the effect of the interaction between the leaching temperature and acid concentration is negative. Increasing the leaching temperature increases the consumption of nitric acid, thereby enhancing the pH of the solution, which could influence the REEs and phosphate leaching efficiencies.

As demonstrated in Fig. 5, at leaching time of 60 min, enhancement of the acid concentration from 35 wt.% to 65 wt.% and the temperature from 24°C to 90°C resulted in the maximum leaching efficiencies of REEs and phosphate. The temperature–acid concentration interaction had a similar impact on the leaching efficiencies of LREEs and HREEs,

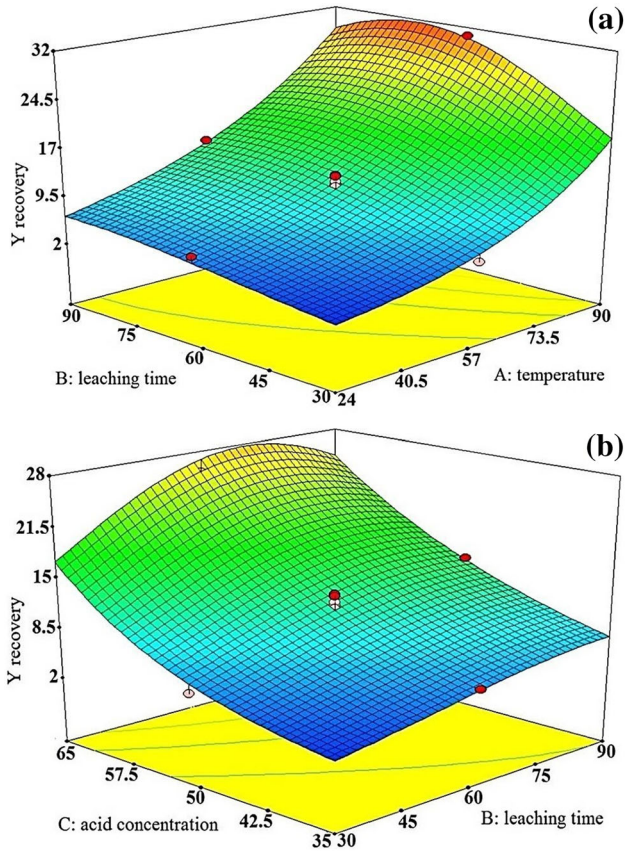

Fig. 6. (a) Effect of interaction between temperature and leaching time on the leaching efficiency of Y (acid concentration 50 wt.%), (b) effect of interaction between acid concentration and leaching time on the leaching efficiency of Y (temperature 57°C). Curves indicate regression models.

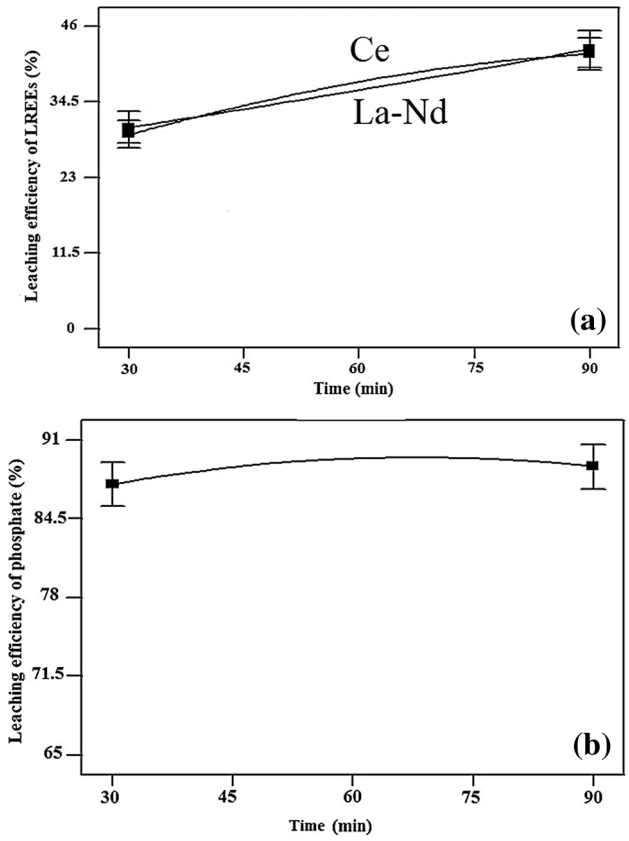

Fig. 7. Effect of leaching time on leaching efficiency of (a) LREEs and (b) phosphate at acid concentration of 65 wt.% and temperature of 90°C. Curves indicate regression models.

which can be attributed to proton activity ($\{H^+\}$) and NO_3^- anion complexation with the calcium of fluorapatite.[17] The following reaction sequence has been proposed to describe the dissolution model of fluorapatite:[23]

$$Ca_5(PO_4)_3(F) + H_2O + H^+ = Ca_5(PO_4)_3(H_2O)^+ + HF \quad (10)$$

$$2Ca_5(PO_4)_3(H_2O)^+ = 3Ca_3(PO_4)_2 + Ca^{2+} + 2H_2O \quad (11)$$

$$Ca_3(PO_4)_2 + 2H^+ = Ca^{2+} + 2CaHPO_4 \quad (12)$$

$$CaHPO_4 + H^+ = Ca^{2+} + H_2PO_4^- \quad (13)$$

The results show that increasing the acid concentration from 50 wt.% to 65 wt.% at leaching time of 60 min and temperature of 57°C elevated the leaching efficiency of total REEs from 15.7% to 25.7%. However, such an increase in acid concentration (at the same conditions of temperature and time) did not significantly increase the leaching efficiency of phosphate (Fig. 5).

Effect of Leaching Time

Equations 5–9 describe the leaching efficiency of Ce, La, Nd, Y, and phosphate. As seen from these relationships, the leaching time had the least impact on the leaching efficiencies of REEs and phosphate. Increasing the leaching time enhanced the leaching efficiency of REEs and phosphate (Figs. 6 and 7). The interactions of the leaching time with the acid concentration and temperature played an important role in the leaching of Y as a HREE. However, the interaction between the leaching temperature and the acid concentration was the only significant interactive effect on the leaching efficiency of LREEs. In Esfordi concentrate, Ce, La, and Nd originate from fluorapatite and monazite minerals, but fluorapatite and xenotime minerals are the origins of Y,[20] which may explain the lower leaching efficiency of Y and the significant effect of the interactions between the leaching time and other factors for Y. It can be deduced from Fig. 6a and b that the maximum leaching efficiency of Y was achieved when using a leaching time of 75 min, temperature of 90°C, and acid concentration of 65%.

The effects of the leaching time on the leaching efficiency of LREEs and phosphate are shown in Fig. 7a and b. As suggested by Fig. 7a, the leaching

efficiency of LREEs increased on prolonging the leaching time. The leaching efficiencies of Ce, La, and Nd followed identical trends. The leaching efficiency of phosphate increased from 87.3% to 89.7% when the leaching time was prolonged from 30 min to 70 min (Fig. 7b). No significant increase in the leaching efficiency of phosphate was observed with prolongation of the leaching time from 70 min to 90 min. Note that the leaching efficiency of calcium and phosphate followed the same trends to some extent. When fluorapatite is leached by nitric acid, calcium, phosphate, and fluoride ions are released into solution as shown in Eqs. 1 and 14.[23] Thus, it can be concluded that the leaching rate of calcium and phosphate will be high in strong acids. Stone et al. (2016) and Soltani et al. (2019) studied the leaching behavior of fluorapatite concentrate in nitric acid and concluded that almost all the calcium and phosphate could be leached in 10 min.[9,24] In Esfordi phosphate concentrate, the part of the phosphate originating from monazite and xenotime refractory minerals cannot be leached at temperatures below 100°C.[15]

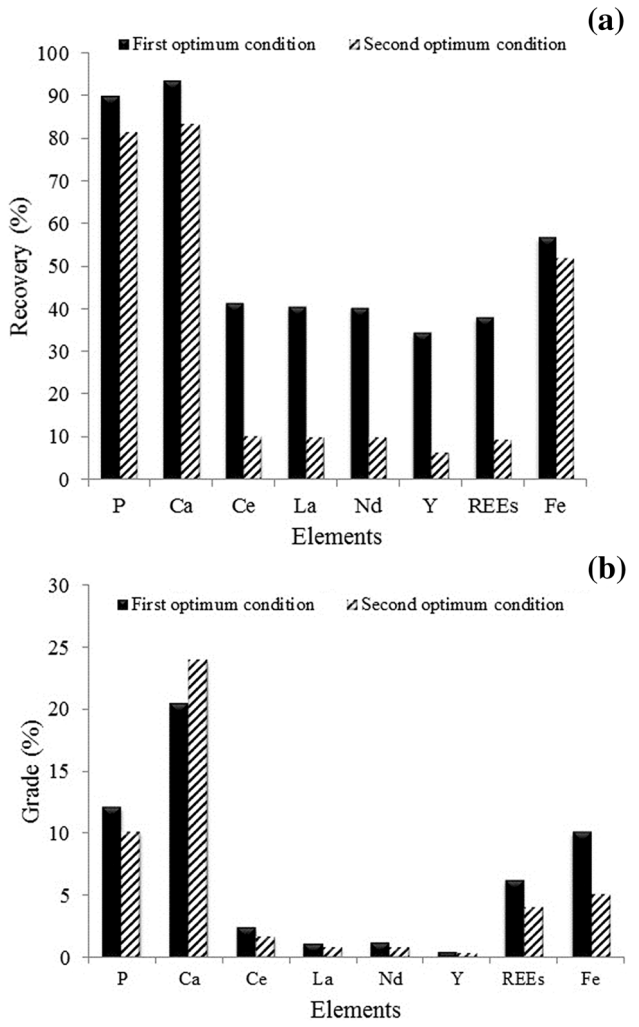

Fig. 8. (a) Leaching efficiency of elements and (b) elemental concentration of leaching residue in both optimum nitric acid leaching conditions.

$$Ca_{10}(PO_4)_6F_2 = 10Ca^{2+} + 6PO_4^{3-} + 2F^- \qquad (14)$$

Although the highest REE leaching efficiency was achieved at longer leaching times and higher acid concentrations, such conditions require high acid consumption, which could adversely affect the economic viability of the leaching process.

Optimum Conditions

The aim of the current optimization is to determine a combination of factors that simultaneously satisfies the requirements placed on each of the responses and factors. For this purpose, two sets of conditions were selected based on the predefined targets: (1) direct leaching of REEs, where conditions were selected to maximize the leaching efficiency of REEs and phosphate; for acid concentration of 65% and leaching time of 81 min at 90°C, the maximum leaching efficiency of REEs and phosphate reached 38.6% and 89.3%, respectively (Fig. 8a); (2) selective leaching of REEs from calcium and phosphate, where for acid concentration of 35% and leaching time of 70 min at 60°C, the leaching efficiency of phosphate and REEs reached 9% and 82.3%, respectively. The proposed optimum

Table V. Optimum conditions for leaching of REEs and phosphate

	Target		Leaching efficiency (%)						Condition		
	REEs Leaching efficiency	**P** Leaching efficiency	**Ce**	**Nd**	**La**	**Y**	**ΣREE**	**P**	**Temperature (°C)**	**Acid con. (%)**	**Time (min)**
1 (fit models)	Max	Max	40.9	40.4	40.7	34.2	38.6	89.3	90	65	81
1 (experiment)	–	–	41.3	40.2	40.3	34.2	37.8	88.5	90	65	81
2 (fit models)	Min	Max	10.5	9.7	9.6	6.1	9	82.3	60	35	70
2 (experiment)	–	–	10	9.8	9.8	6.2	9.3	81.7	60	35	70

conditions were validated by confirmation experiments, as presented in Table V.

In the first case of optimization, the concentrations of REEs, calcium, and phosphorus in the leach solution were 2752 mg/L, 216,752 mg/L, and 78,645 mg/L, respectively. Due to the presence of high levels of phosphate, calcium, and REEs in the pregnant leach solution, calcium removal is necessary prior to recovery of REEs from the solution. Alemrajabi et al. (2017) showed that calcium can be separated from nitrophosphoric solutions by cooling crystallization to $Ca(NO_3)_2{\cdot}4H_2O$. The solution is then neutralized using ammonia, so the REEs precipitate mainly as phosphates.[10]

In the second case of optimization, 90.7% of the REEs remained in the residue and the grade of REEs in the residue was increased from 1.09% to 4% (Fig. 8b). In this condition, the phosphate and calcium recoveries of the residue were less than 20%. This residue is an appropriate feed for the acid baking process, as it has low calcium content. In this way, a phosphoric acid solution and REE-concentrated residue can be produced. Therefore, a selective leaching stage can be used to leach calcium and phosphate from the concentrate prior to the acid baking process.

CONCLUSION

Esfordi phosphate concentrate with 34.6% Ca, 13.1% P, 2.58% Fe, and 1.09% total REEs was selectively leached with nitric acid, and the effects of the acid concentration, reaction time, and temperature were investigated. Based on the results, it can be concluded that use of 35% nitric acid at 60°C for leaching time of 70 min could result in selective leaching of 83% of the calcium and 90% of the phosphate from the concentrate; about 90% of the REEs remained in the leaching residue. Therefore, a nitrophosphate solution and REE-concentrated residue were obtained. The leaching residue could be an appropriate feed for the acid baking process due to its low calcium content. Moreover, calcium in the nitrophosphate solution could be precipitated as gypsum by adding sulfuric acid. In this way, gypsum precipitation and dissolution of REEs could be carried out in two separate steps.

ACKNOWLEDGEMENTS

This project was supported by Iranian Mines and Mining Industries Development and Renovation Organization (Grant No. 9413560201), Iran Mineral Processing Research Center (Grant No. 9413560201), and University of Kashan (Grant No. 9413560201).

REFERENCES

1. M.K. Jha, A. Kumari, R. Panda, J.R. Kumar, K. Yoo, and J.Y. Lee, *Hydrometallurgy* 165, 2 (2016).
2. J. Zhang, B. Zhao, and B. Schreiner, *Separation Hydrometallurgy of Rare Earth Elements*, ed. J. Zhang, B. Zhao, and B. Schreiner (Cham: Springer, 2016), pp. 55–78.
3. A. Jordens, Y.P.C. Kristian, and E. Waters, *Miner. Eng.* 41, 97 (2012).
4. X. Feng, D. Dreisinger, and F. Doyle, *Miner. Eng.* 56, 10 (2014).
5. K. Kawatra and J.T. Carlson, *Soc. Min. Metall. Explor. (SME)* 9, 9 (2014).
6. Z. Ismail, E. Elgoud, F. Hai, O. Ibraheem, A. Gasser, and H. Aly, *Arab. J. Nucl. Sci. Appl.* 48, 37 (2015).
7. C.K. Gupta and N. Krishnamurthy, *Extractive Metallurgy of Rare Earth* (CRC Press, Boca Raton, 2005).
8. L. Wang, Z. Long, X. Huang, Y. Yu, D. Cui, and G. Zhang, *Hydrometallurgy* 101, 41 (2010).
9. K. Stone, A. Bandara, G. Senanayake, and S. Jayasekera, *Hydrometallurgy* 163, 137 (2016).
10. M. Alemrajabi, Å.C. Rasmuson, K. Korkmaz, and K. Forsberg, *Hydrometallurgy* 169, 253 (2017).
11. E. Jorjani, A.H. Bagherieh, and S.C. Chelgani, *Korean J. Chem. Eng.* 28, 557 (2011).
12. S. Wu, L. Wang, L. Zhao, P. Zhang, H. El-Shall, B. Moudgil, X. Huang, and L. Zhang, *Chem. Eng. J.* 335, 774 (2018).
13. F. Habashi, *Can Metall. Q.* 52, 229 (2013).
14. L. Hongfei, G. Fuqiang, Z. Zhifeng, L. Deqian, and W. Zhonghuai, *J. Alloys Compd.* 408, 995 (2005).
15. F. Soltani, M. Abdollahy, S.M. Javad Koleini, and D. Moradkhani, *J. South Afr. Inst. Min. Metall.* 117, 443 (2017).
16. K.M Forsberg, M. Mohammadi, S. Ghafarnejad Parto, D.L.C.J. Martinez, Å. Rasmuson, and A. Fredriksson, Recovery of REE from an apatite concentrate. In *53rd Conference of Metallurgists*, Vancouver, Canada (2014).
17. A. Bandara and G. Senanayake, *Hydrometallurgy* 153, 179 (2015).
18. D.C. Montgomery, *Design and Analysis of Experiments*, 18th edn. Arizona State University (2013).
19. J.V. Mehrabani, M. Noaparast, S.M. Mousavi, R. Dehghan, and A. Ghorbani, *Sep. Purif. Technol.* 72, 242 (2010).
20. F. Soltani, M. Abdollahy, J. Petersen, R. Ram, M. Becker, S.M. Javad Koleini, and D. Moradkhani, *Hydrometallurgy* 177, 66 (2018).
21. H. Li, F. Guo, Z. Zhang, D. Li, and Z. Wang, *J. Alloys Compd.* 408, 995 (2006).
22. Y.M. Khawassek, A.A. Eliwa, E.A. Gawad, S.M. Abdo, and J. Rad, *Res. Appl. Sci.* 8, 583 (2015).
23. S.V. Dorozhkin, *World J. Methodol.* 2, 1 (2012).
24. F. Soltani, M. Abdollahy, J. Petersen, R. Ram, S.M. Javad Koleini, and D. Moradkhani, *Hydrometallurgy* 184, 73 (2019).